Dynamic Preshaping Based Design of Capturing Robot Driven by Wire

Shoichi NISHIO*, Mitsuru HIGASHIMORI*, and Makoto KANEKO*

*Graduate School of Engineering, Hiroshima University, Higashi-Hiroshima 739-8527, JAPAN

Abstract

This paper discusses the design of wire drive capturing robots based on dynamic preshaping. As the speed of a robot hand increases, dynamic effects become dominant. In order to successfully catch an object by a high speed capturing robot, it is important to consider mass distribution, wiring, and joint spring when designing the robot. After explaining the design procedure by considering those mechanical parameters, experiments as well as simulations are shown to verify the basic idea.

1 Introduction

While a number of robots have been developed so far, we are particularly interested in high speed robots that can capture a moving object quickly. As the first trial of such a high speed robot, we have designed and developed the 100G capturing robot[1] that can catch a flying object in the air within the motion time of 50[msec]. Fig.1 shows an experimental result where the 100G capturing robot is capturing a ball by the gripper. Due to such a high speed, we cannot follow by our eyes what is really happening during the capturing motion. Therefore, we can not see directly why the robot fails in catching the object while it looks like that the gripper successfully reaches the target object position. After precise analysis utilizing a high speed camera with the frame rate of 1[msec], we found that the preshape of the gripper is not appropriate, especially for the final stage of catching motion. Considering the finger link posture during the high speed capturing motion, it is impossible to neglect inertia force applied to the finger links. Therefore, the preshaping issue under such a high speed condition results in an optimum design problem to determine the joint torque distribution with considering the effects of dynamics. The goal of this work is to provide a design procedure on preshaping issue for a high speed capturing robot.

Reducing mass of the robot is really important for achieving a high acceleration. In such sense, wire drive robots are good candidates for reducing mass of both arm and gripper, since we can install all actuators at the base. We suppose a robot where all joints are controlled by a single wire. A feature of such robots is that the torque distribution is determined by both the size of pulley in each joint and the way of wiring. By focusing on such a wire drive robot, we define that the dynamic preshaping problem is to produce a joint torque set so that all links make contact with an object. We explore the geometrical issue where the design for wiring is precisely discussed. After explaining the design procedure for achieving the reference posture under high speed condition by considering mechanical parameters of the robot, experiments as well as simulations are shown to verify the basic idea.

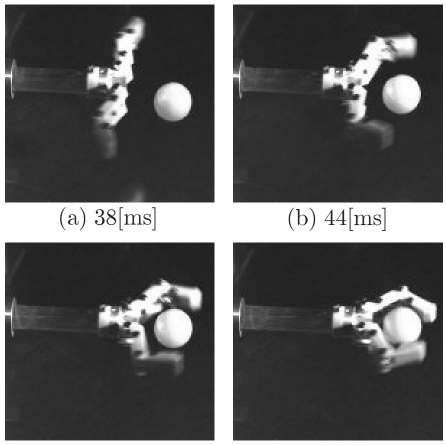

(a) 38[ms] (b) 44[ms] (c) 46[ms] (d) 48[ms]

Fig. 1: A two-fingered robot hand for capturing an object.

2 Related Works

There have been a couple of works discussing preshaping issues so far[3]–[8]. Bard and Troccaz[3] have discussed an automatic preshaping for a dexterous hand from a single description of objects, where the object model is automatically extracted from a low-level visual data and a system for preshaping a planar two-fingered hand with four joints grasping planar ob-

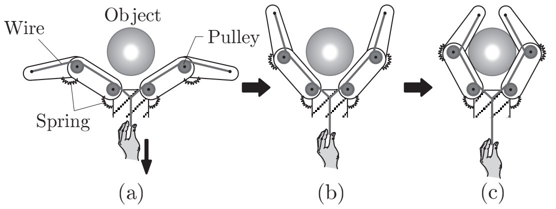

Fig. 2: Basic mechanism of a high speed capturing robot driven by a single wire.

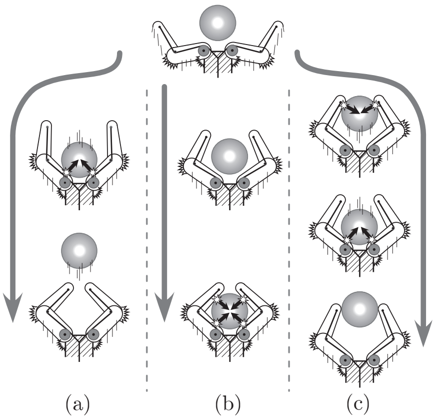

Fig. 3: Various behaviors of object when finger links make contact with it.

jects is described. Kang and Ikeuchi[4] have proposed an automatic robot instruction for recognizing a grasp from observation. Hong and Slotine[5] have proposed a catching algorithm by which they succeeded in real time catching free-flying spherical balls being tossed from random locations. The postures of the robot hand and arm at the moment of capturing are planned by the information obtained by vision. Nakamura et. al. [6] have challenged the reactive grasp of a three-fingered robot hand by using a learning method, where the preshaping is planned by integrating 48 kinds of sensor signals and 29 primitive behaviors. As far as we know, our paper is the first work discussing dynamic preshaping.

3 Problem Formulation

3.1 Robot Hand Driven by a Single Wire

Suppose a typical robot hand where each actuator is placed at each joint. In such a case, the whole weight of the robot increases and the motion of the robot becomes slow as a result. In order to decrease the weight, the wire drive method where all actuators are arranged at the base of the robot and the torque driving each joint is transmitted through wire, has been utilized[1][2]. Consider a multi-linked robot hand where all joints are controlled by a single wire, as shown in Fig.2. Now we focus on only open-close motion of fingers. The motions of the arm are ignored. Since all joints of the robot are driven by the tension of one control wire[1], the distribution of drive torque for each joint is determined by the wiring, i.e., pulley position and radius. In addition, a spring is attached to each joint to keep the initial link posture when wire tension is zero. This spring produces a resistant force for the joint torque coming from wire tension.

3.2 Reference Posture

Suppose a capturing robot trying to capture an object, as shown in Fig.3, where (a) and (c) are examples of failure in catching an object, and (b) is an example of successful catching, respectively. From the geometrical point of view, it is more likely that the simultaneous contact between links and the object leads to a successful catching. Based on this consideration, we define the reference posture of finger links as shown in Fig.3(b), and this is given by following.

Reference Posture: The reference posture is given by the grasping form where all links make contact with an object, and is expressed by the joint angular vector $\boldsymbol{\theta}_r \in \mathcal{R}^{\Sigma_{s=1}^{U} N_s \times 1}$, where U and N_s denote the number of fingers and the number of joints (= the number of links) of the s-th finger, respectively.

3.3 Dynamic Preshaping Problem

In this work, we suppose that capturing motions by robot hands can be regarded as realizing the given reference posture $\boldsymbol{\theta}_r$. We define the dynamic preshaping problem as follwing.

Dynamic Preshaping Problem: By giving the reference joint angle $\boldsymbol{\theta}_r$, determine the mechanical parameters (pulley radius, pulley position, spring constant, and mass of finger link), so that the following condition is satisfied.

$$\Delta t_{\theta_r} = \max \left| \, t_{\theta_{sir}} - t_{\theta_{sjr}} \right| < \varepsilon \qquad (1)$$
$$(s = 1, \ldots, U, \; i = 1, \ldots, N_s, \; j = 1, \ldots, N_s)$$

where $t_{\theta_{sir}}$ denotes the time when the i-th joint of the s-th finger reaches the reference angle and ε is a small positive value.

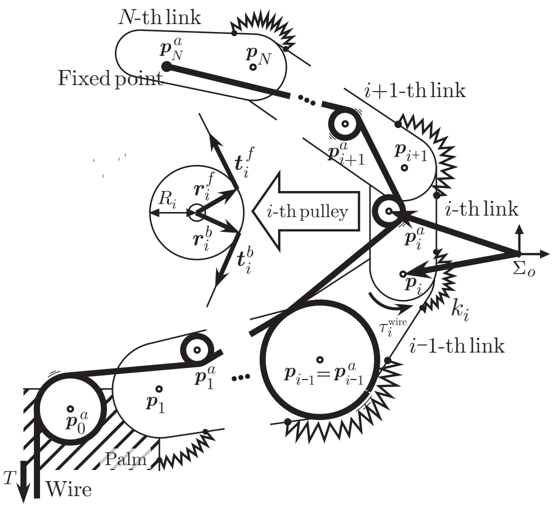

Fig. 4: A 2D finger model driven by a single wire.

4 Mechanical Analysis

4.1 Wiring

Suppose a 2D finger is driven by a single wire as shown in Fig.4, where $\boldsymbol{p}_i$, $\boldsymbol{p}_i^a$, and $\boldsymbol{p}_N^{fix} \in \mathcal{R}^{2\times 1}$ are the position vectors expressing the i-th joint position, the i-th pulley position at inner link, and the wire fixing point at the N-th link, respectively, and all pulleys can be freely rotated around their axes. $\boldsymbol{p}_0^a$ is the position vector expressing the pulley position at the palm, and whole link system is fixed with the base at $\boldsymbol{p}_1$. Let $\boldsymbol{t}_i^f \in \mathcal{R}^{2\times 1}$ and $\boldsymbol{t}_i^b \in \mathcal{R}^{2\times 1}$ be the tension vectors before and after the i-th pulley, respetively, as shown Fig.4. Supposing that there is no friction around each pulley axis, we have $\|\boldsymbol{t}_i^b\| = \|\boldsymbol{t}_i^f\| = T$ where T is the wire tension. Also, let $\boldsymbol{r}_i^f \in \mathcal{R}^{2\times 1}$ and $\boldsymbol{r}_i^b \in \mathcal{R}^{2\times 1}$ be the vectors denoting the positions where the wire tensions are given. Under the above preparation, we have the following relationship.

$$\boldsymbol{t}_i^f = -\boldsymbol{t}_{i+1}^b \tag{2}$$

$$\boldsymbol{r}_i^b \otimes \boldsymbol{t}_i^b = -\boldsymbol{r}_i^f \otimes \boldsymbol{t}_i^f \tag{3}$$

where $\otimes$ denotes the operator providing $x_1y_2 - x_2y_1$ for two vectors $\boldsymbol{x} = [x_1, x_2]^{\mathrm{T}}$ and $\boldsymbol{y} = [y_1, y_2]^{\mathrm{T}}$. By letting $\boldsymbol{d}_i^{i+1} \in \mathcal{R}^{2\times 1}$ express the vector from the wire release point of the i-th pulley to that of the $i+1$-th pulley, we get

$$\boldsymbol{p}_{i+1}^a = \boldsymbol{p}_i^a + \boldsymbol{r}_i^f + \boldsymbol{d}_i^{i+1} - \boldsymbol{r}_{i+1}^b \tag{4}$$

By multiplying $\otimes \boldsymbol{t}_{i+1}^b$ by right side to each term on eq.(4) and considering $\boldsymbol{d}_i^{i+1} \otimes \boldsymbol{t}_{i+1}^b = 0$, we obtain the following equation:

$$(\boldsymbol{p}_{i+1}^a - \boldsymbol{p}_i^a) \otimes \boldsymbol{t}_{i+1}^b = (\boldsymbol{r}_i^f - \boldsymbol{r}_{i+1}^b) \otimes \boldsymbol{t}_{i+1}^b \tag{5}$$

The torque around the i-th joint is given by the following form:

$$\tau_i^{\mathrm{wire}} = (\boldsymbol{p}_i^a - \boldsymbol{p}_i) \otimes \boldsymbol{t}_i^b + (\boldsymbol{p}_i^a - \boldsymbol{p}_{i+1}) \otimes \boldsymbol{t}_i^f \tag{6}$$

From eqs.(2), (3), (5), and (6), τ_i^{wire} can be rewritten with $\boldsymbol{r}_i^b$ by the following form.

$$\tau_i^{\mathrm{wire}} = T R_i^{vp} \tag{7}$$

where

$$\begin{aligned} R_i^{vp} &= (\boldsymbol{p}_i^a - \boldsymbol{p}_i + \boldsymbol{r}_i^b) \otimes \boldsymbol{e}_i^b \\ &\quad -(\boldsymbol{p}_{i+1}^a - \boldsymbol{p}_{i+1} + \boldsymbol{r}_{i+1}^b) \otimes \boldsymbol{e}_{i+1}^b \end{aligned} \tag{8}$$

Let $\boldsymbol{e}_i^b (= \boldsymbol{t}_i^b / T) \in \mathcal{R}^{2\times 1}$ be the unit vector expressing the direction of tension. Eq.(7) means that the torque produced by a wire can be expressed by the multiplying the wire tension with the radius of virtual pulley. We would note that the radius of such a virtual pulley varies depending upon the link posture.

The above discussions provide us with the relationship between the torque and the wire tension in the following form:

$$\boldsymbol{\tau}^{\mathrm{wire}} = T\,[\boldsymbol{A} + \boldsymbol{B}]\,\boldsymbol{e}^b \tag{9}$$

where

$$\boldsymbol{\tau}^{\mathrm{wire}} = \left[\tau_1^{\mathrm{wire}}, \cdots, \tau_N^{\mathrm{wire}}\right]^{\mathrm{T}} \in \mathcal{R}^{N\times 1} \tag{10}$$

$$\boldsymbol{A} = \begin{bmatrix} [\boldsymbol{q}_1 \otimes] & -[\boldsymbol{q}_2 \otimes] & & \boldsymbol{0} \\ & & \ddots & \\ & & [\boldsymbol{q}_{N-1} \otimes] & -[\boldsymbol{q}_N \otimes] \\ \boldsymbol{0} & & & [\boldsymbol{q}_N \otimes] \end{bmatrix} \in \mathcal{R}^{N\times 2N} \tag{11}$$

$$\boldsymbol{q}_i = \boldsymbol{p}_i^a - \boldsymbol{p}_i \in \mathcal{R}^{2\times 1} \tag{12}$$

$$\boldsymbol{B} = \begin{bmatrix} [\boldsymbol{r}_1^b \otimes] & -[\boldsymbol{r}_2^b \otimes] & & \boldsymbol{0} \\ & & \ddots & \\ & & [\boldsymbol{r}_{N-1}^b \otimes] & -[\boldsymbol{r}_N^b \otimes] \\ \boldsymbol{0} & & & [\boldsymbol{r}_N^b \otimes] \end{bmatrix} \in \mathcal{R}^{N\times 2N} \tag{13}$$

$$\boldsymbol{e}^b = \left[\boldsymbol{e}_1^{b\,\mathrm{T}}, \cdots, \boldsymbol{e}_N^{b\,\mathrm{T}}\right]^{\mathrm{T}} \in \mathcal{R}^{2N\times 1} \tag{14}$$

where $[\boldsymbol{x}\otimes]$ means $[-x_2, x_1] \in \mathcal{R}^{1\times 2}$ for a vector $\boldsymbol{x} = [x_1, x_2]^{\mathrm{T}}$. $\boldsymbol{A}\boldsymbol{e}^b$ and $\boldsymbol{B}\boldsymbol{e}^b$ express the torque components controlled by the position of pulley and by both the radius of pulley and the way of wiring, respectively.

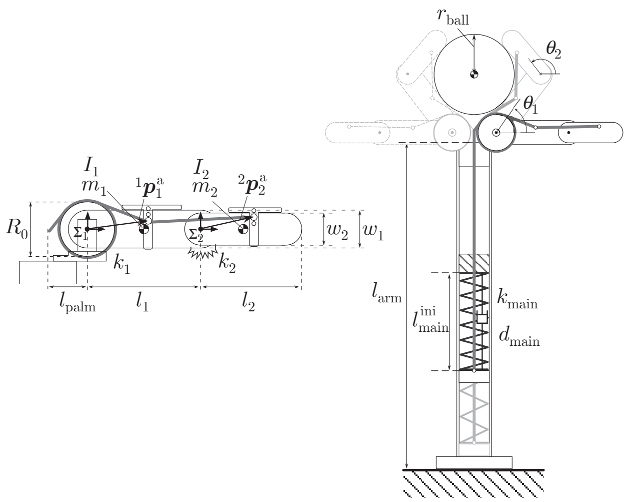

Fig. 5: Finger model for determining parameters.

Table 1: Mechanical parameters used for simulation.

l_1	length of the 1st link	60.0[mm]
l_2	length of the 2nd link	45.0[mm]
m_1	mass of the 1st link	55.0[g]
m_2	mass of the 2nd link	30.0[g]
I_1	moment of inertia of the 1st link	27.6[kgmm^2]
I_2	moment of inertia of the 2nd link	7.1[kgmm^2]
w_1	width of the 1st link	20.0[mm]
w_2	width of the 2nd link	17.0[mm]
l_{palm}	position of the 1st joint	10.0[mm]
l_{arm}	length of arm	260.0[mm]
$l_{\text{main}}^{\text{ini}}$	initial length of main spring	70.0[mm]
k_{main}	spring constant of main spring	0.60[N/mm]
d_{main}	damping coefficient of main spring	0.01[Ns/mm]
$l_{k_{\text{main}}}$	natural length of main spring	180.0[mm]
r_{ball}	radius of object	32.5[mm]
θ_1^{ini}	initial angle of the 1st joint	0.0[rad]
θ_2^{ini}	initial angle of the 2nd joint	0.0[rad]
k_1	spring constant of the 1st joint	90.0[Nmm/rad]
k_2	spring constant of the 2nd joint	120.0[Nmm/rad]
R_0	radius of base pulley	15.0[mm]
R_1	radius of pulley on the 1st link	0.01[mm]

4.2 Joint Compliance

Let us now consider the effect of spring distribution among joints, where k_i is the i-th joint spring constant as shown in Fig.4. Each joint spring plays an important role for controlling the finger link posture when the fingers approach an object. We have the following relationship between the joint torque and spring constant.

$$\boldsymbol{\tau}^{\text{spring}} = -\boldsymbol{Q}\boldsymbol{k} \tag{15}$$

where

$$\boldsymbol{\tau}^{\text{spring}} = \left[\tau_1^{\text{spring}}, \cdots, \tau_N^{\text{spring}}\right]^{\text{T}} \in \mathcal{R}^{N\times 1} \tag{16}$$

$$\boldsymbol{Q} = \begin{bmatrix} \theta_1 \ \theta_1-\theta_2 & & & \boldsymbol{0} \\ & \ddots & & \\ & \theta_i-\theta_{i-1} & \theta_i-\theta_{i+1} & \\ & & \ddots & \\ \boldsymbol{0} & & & \theta_N-\theta_{N-1} \end{bmatrix} \in \mathcal{R}^{N\times N} \tag{17}$$

$$\boldsymbol{k} = [k_1, \cdots, k_N]^{\text{T}} \in \mathcal{R}^{N\times 1} \tag{18}$$

4.3 Equation of Motion

The equation of motion of the finger link system can be modeled by the following,

$$\boldsymbol{M}(\boldsymbol{\theta})\ddot{\boldsymbol{\theta}} + \boldsymbol{h}(\dot{\boldsymbol{\theta}}, \boldsymbol{\theta}) = \boldsymbol{\tau}^{\text{wire}} + \boldsymbol{\tau}^{\text{spring}} \tag{19}$$

where $\boldsymbol{M}(\boldsymbol{\theta}) \in \mathcal{R}^{N\times N}$ and $\boldsymbol{h}(\dot{\boldsymbol{\theta}}, \boldsymbol{\theta}) \in \mathcal{R}^{Ns\times 1}$ are the inertia matrix and velocity related torque vector, respectively. From eqs.(9) and (15), eq.(19) can be rewritten in the following form:

$$\boldsymbol{M}(\boldsymbol{\theta})\ddot{\boldsymbol{\theta}} + \boldsymbol{h}(\dot{\boldsymbol{\theta}}, \boldsymbol{\theta}) = T\left[\boldsymbol{A}(\boldsymbol{\theta}) + \boldsymbol{B}(\boldsymbol{\theta})\right]\boldsymbol{e}^b(\boldsymbol{\theta}) - \boldsymbol{Q}(\boldsymbol{\theta})\boldsymbol{k} \tag{20}$$

5 Dynamic Preshaping

5.1 Parameter Determination

Since the equation of motion given by eq.(20) is highly nonlinear, it is really difficult to formulate an algorithm for solving the dynamic preshaping problem. Through the analysis of wiring, we learnt that each joint torque is very sensitive to the pulley position and even negative torque can be generated according to the location, while it is hard to achieve such a characteristic by changing either spring constant or mass distribution. Based on these considerations, let us now replace the problem obtaining the mechanical parameters for realizing $\boldsymbol{\theta}_r$ by the following optimization problem.

Minimize

$$Z = \Delta t_{\theta_r}$$

Subject to

$$ {}^i\boldsymbol{p}_i^{a\min} \le {}^i\boldsymbol{p}_i^{a} \le {}^i\boldsymbol{p}_i^{a\max} \quad (i = 1, \ldots, N)$$
$$\boldsymbol{M}(\boldsymbol{\theta})\ddot{\boldsymbol{\theta}} + \boldsymbol{h}(\dot{\boldsymbol{\theta}}, \boldsymbol{\theta}) = T\left[\boldsymbol{A}(\boldsymbol{\theta}) + \boldsymbol{B}(\boldsymbol{\theta})\right]\boldsymbol{e}^b(\boldsymbol{\theta}) - \boldsymbol{Q}(\boldsymbol{\theta})\boldsymbol{k}$$

where ${}^i\boldsymbol{p}_i^{a\min}$ and ${}^i\boldsymbol{p}_i^{a\max} \in \mathcal{R}^{2\times 1}$ are the minimum and the maximum limitations of the pulley position, respectively. Now, the evaluation function Z is corresponding to eq.(1).

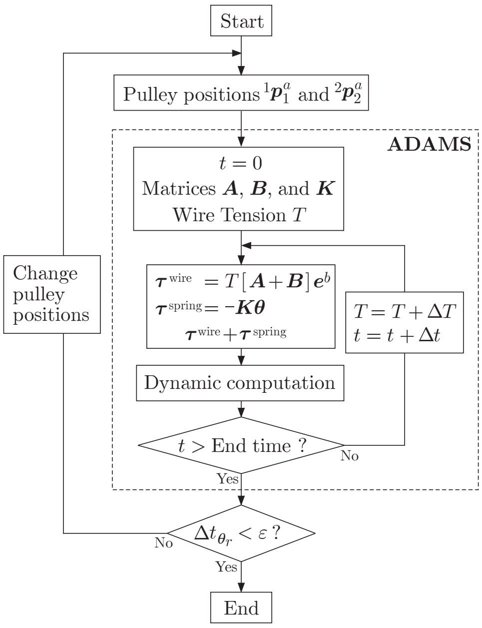

Fig. 6: Flow chart for computing the pulley positions.

5.2 Simulations

In order to obtain the pulley position satisfying the condition expressed by eq.(1), we repeat computation until it converges. Consider a two-fingered hand and a sphere object as shown in Fig.5. All parameters except for $^1\boldsymbol{p}_1^a$ and $^2\boldsymbol{p}_2^a$ are given by Table.1. We also suppose that one tip of the wire is fixed at the one side of the spring implemented in the arm and the other tip of wire is fixed at the second finger link. We assume that the wire tension T is generated by the following equation.

$$T = k_{\text{wire}}\Delta l_{\text{wire}} - d_{\text{wire}}\Delta \dot{l}_{\text{wire}} \tag{21}$$

where k_{wire}, d_{wire}, and Δl_{wire} are virtual stiffness, damping coefficient, and the amount of stretch, respectively. Now, we give $k_{\text{wire}} = 1.0 \times 10^6$[N/mm] and $d_{\text{wire}} = 1.0 \times 10^{-2}$[Ns/mm]. We also suppose that the friction between each finger link and the object is given by $\mu = 0.0$. The dynamic simulator ADAMS (Mechanical Dynamics, Inc.) is utilized for computing finger motion for a given set of parameters. Fig.6 shows the flow chart for computing the pulley positions $^1\boldsymbol{p}_1^a$ and $^2\boldsymbol{p}_2^a$ in Fig.5 for achieving the reference finger posture at the instance of contact. Fig.7 shows two simulation results where (a) and (b) are $\varepsilon = 13$[ms] and $\varepsilon = 0.4$[ms], respectively. In case of $\varepsilon = 13$[ms], we obtain the optimum pulley positions $^1\boldsymbol{p}_1^a = [32.0, 2.0]^{\mathrm{T}}$[mm] and $^2\boldsymbol{p}_2^a = [25.0, 2.5]^{\mathrm{T}}$[mm].

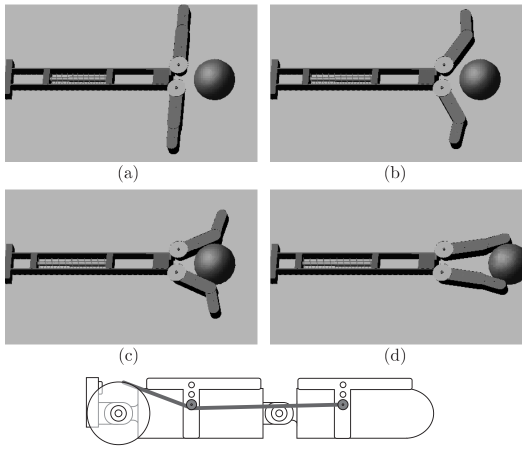

(a) $^1\boldsymbol{p}_1^{\mathrm{a}} = [32.0 \ \ 2.0]^{\mathrm{T}}$[mm] , $^2\boldsymbol{p}_2^{\mathrm{a}} = [25.0 \ \ 2.5]^{\mathrm{T}}$[mm]

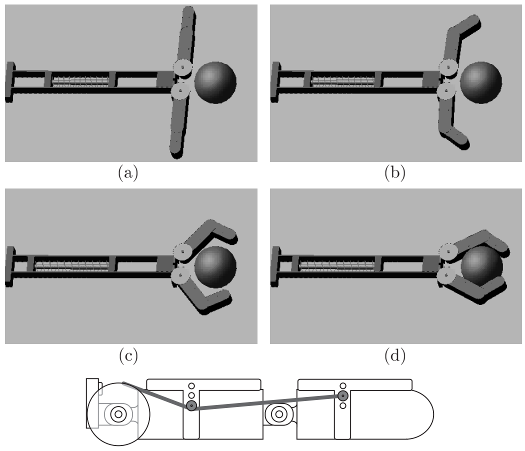

(b) $^1\boldsymbol{p}_1^{\mathrm{a}} = [32.0 \ \ 2.0]^{\mathrm{T}}$[mm] , $^2\boldsymbol{p}_2^{\mathrm{a}} = [25.0 \ \ 6.5]^{\mathrm{T}}$[mm]

Fig. 7: Simulation results for two different sets of pulley position.

As shown in Fig.7(a), the first link makes contact with the object earlier than the second one and the object is finally pushed away. This result suggests that $\varepsilon = 13$[ms] is not small enough. In case of $\varepsilon = 0.4$[ms], we obtain $^1\boldsymbol{p}_1^a = [32.0, 2.0]^{\mathrm{T}}$[mm] and $^2\boldsymbol{p}_2^a = [25.0, 6.5]^{\mathrm{T}}$[mm] after convergence. In this case, all links make contact with the object with in 1[ms]. As shown in Fig.7(b), the robot can capture the object successfully while it includes a small oscillational motion.

6 Experiments

We designed and developed an experiment system for confirming the simulation results, where we can change the wiring route by changing the pulley posi-

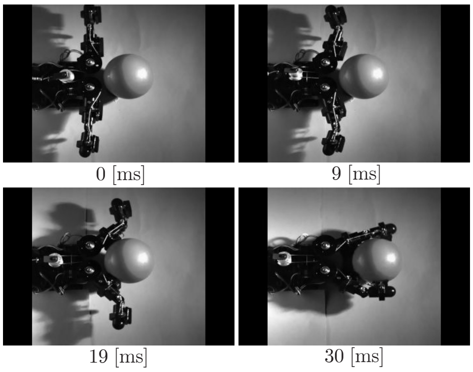

(a) ${}^1\boldsymbol{p}_1^{\mathrm{a}} = [32.0\ \ 2.0]^{\mathrm{T}}$[mm] , ${}^2\boldsymbol{p}_2^{\mathrm{a}} = [25.0\ \ 2.5]^{\mathrm{T}}$[mm]

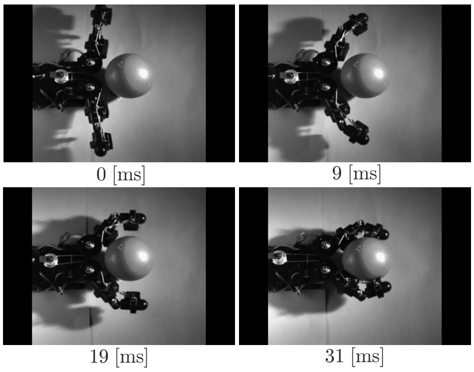

(b) ${}^1\boldsymbol{p}_1^{\mathrm{a}} = [32.0\ \ 2.0]^{\mathrm{T}}$[mm] , ${}^2\boldsymbol{p}_2^{\mathrm{a}} = [25.0\ \ 6.5]^{\mathrm{T}}$[mm]

Fig. 8: Experimental results for two different sets of pulley position.

tion and the pulley size, the joint spring constant, and the mass distribution of the links, respectively. The tension of the wire is generated by the elastic energy of the spring mounted in the arm. Mechanical parameters except for the pulley positions are given by Table.1 where parameter explanation is given in Fig.5. We observe the change of the link posture by shifting the pulley positions along the simulation results. Fig.8 shows a series of photo taken by a high-speed camera with 1 [ms/frame], where the hand is taking action for capturing a sphere object. The hand as shown in Fig.8(a) and (b) are designed under the pulley position as shown in Fig.7(a) and (b), respectively. While the first link makes contact with the object earlier than the second one in Fig.8(a), all links almost make contact with the object simultaneously in Fig.8(b). From Fig.8, we can see that the behaviors of finger links in the simulation and experiment nicely coincide. Therefore, the validity of the optimum parameters obtained by the simulation are supported by experiments.

7 Concluding Remarks

We discussed the design of capturing robot driven by a wire from the viewpoint of dynamic preshaping. The main results are summarized as follows;

(1) Dynamic preshaping is important, especially just before finger links make contact with the object. We choose the preshape so that all links make contact with the object simultaneously.

(2) The mechanical parameters which influences joint drive torque were considered and the relationship between the wire tension and the joint torque distribution was introduced precisely.

(3) The design procedure for achieving the reference posture under dynamic condition was explained. A couple of simulations were executed to obtain the optimum parameter and the validity is confirmed experimentally.

This work was supported by CREST of JST (Japan Science and Technology). We are very thankful for the support.

References

[1] M. Kaneko, R. Takenaka, M. Higashimori A. Namiki and M. Ishikawa: "The 100G Capturing Robot –Too Fast to See–," IEEE/ASME Trans. on Mechatronics, vol.8, no.1, pp.37-44, 2003.

[2] S. Hirose and Y. Umetani: "Soft Gripper," Proc. of ISIR, pp.112–127, 1983.

[3] C. Bard and J. Troccaz: "Automatic Preshaping for a Dexterous Hand from a Single Description of Objects," IEEE Proc. of Int. Workshop Intelligent Robots and Systems, pp.865–872, 1990.

[4] S. B. Kang and K. Ikeuchi: "Toward Automatic Robot Instruction from Perception–Recognizing a Grasp from Observation," IEEE Trans. on Robotics and Automation, vol.9, pp.432–443, Aug, 1993.

[5] W. Hong and J.E. Slotine: "Experiments in Hand-Eye Coordination Using Active Vision," Proc. of the 4th Int. Symp. of Experimental Robotics, pp.130–139, 1995.

[6] Y. Nakamura, T. Yamazaki and N. Mizushima: "Motion Synthesis, Learning and Abstraction through Parameterized Smooth Map from Sensors to Behaviors," Proc. of the Int. Symp. of Robotics Research, pp.69–80, 1998.

[7] L. Deman, A. Konno and M. Uchiyama: "Flexible Manipulator Trajectory Learning Control with Input Preshaping Method," Proc. of the 38th SICE Annual Conf. Int., pp.967–972, 1999.

[8] A. Namiki and M. Ishikawa: "Optimal Grasping Using Visual and Tactile Feedback," IEEE Proc. Int. Conf. on Multisensor Fusion and Integration for Intelligent Systems, pp.584–596, 1996.